

Statistics of quantum recurrences in the Hilbert space

A. Iomin^a and G.M. Zaslavsky^{b,c}

^a Department of Physics, Technion, Haifa, 32000, Israel

^b Courant Institute of Mathematical Sciences, New York University, 251 Mercer Str., New York, NY 10012

^c Department of Physics, New York University, 2-4 Washington Place, New York, NY 10003

(Dated: November 2, 2019)

Statistics of Poincaré recurrences in the Hilbert space for a quantum kicked rotor is studied. A strong correlation between classical accelerator mode dynamics in the phase space and statistics of the quantum recurrences (QR) in the Hilbert space is found. It is shown numerically that the appearance of accelerator mode islands (AMI) by bifurcation leads to power law distribution of the QR in the Hilbert space. Conversely, for chaotic dynamics, when the AMI are absent or their influence is negligible, the QR have an exponential distribution.

PACS numbers: 05.45.Mt

Statistics of Poincaré recurrences is a powerful method for studying anomalous transport in chaotic systems with generic phase space structures, where regular and chaotic regions coexist [1]. The reason is that the distribution of the Poincaré cycles (recurrence time) is sensitive to the topological structure of the phase space and to the probabilistic features of chaotic trajectories. Particularly, for the chaotic systems with a uniform mixing property, the distribution is exponential [2]

$$P(\tau) = \frac{1}{\tau_{\text{rec}}} \exp(-\tau/\tau_{\text{rec}}) \quad (1)$$

with the mean recurrence time

$$\tau_{\text{rec}} = \frac{1}{h_0} \int_0^\infty P(\tau) d\tau = 1/h_0; \quad (2)$$

where h_0 is a metric entropy. It follows, due to the Kac lemma, that $\tau_{\text{rec}} < 1/h_0$ for the area preserving and bounded dynamics [3]. In systems with nonuniform mixing and sticky island regions, distribution of recurrences can be algebraic in the asymptotics of the large times recurrences:

$$P(\tau) \sim 1/\tau^\alpha; \quad (\alpha > 1); \quad (3)$$

where α is called the recurrence exponent [1]. From the Kac lemma it follows that $\alpha > 2$ [3] (see also [4, 5]). Distribution of the Poincaré recurrences is therefore proven to be a powerful method for verification of the space-time complexity in classical Hamiltonian dynamics with nonzero or zero Lyapunov exponents or systems that exhibit a strong intermittent behavior with flights, trapings, weak mixing, etc. See [6] and references therein.

In quantum systems the classical methodology fails because of the absence of trajectories, and any possible generalization of the notion of the Poincaré recurrences is desirable, although it can be nonunique. It is worthwhile to mention that, for systems with chaotic dynamics, a sequence of recurrence times $\tau_{\text{rec}} = \tau_1; \tau_2; \dots; \tau_{\text{rec}}$ is a stochastic process with properties which depend on the type of dynamics. One can expect a similar process in the quantum case, which should not be confused with the phenomenon of periodic revivals of the wave functions [7].

In this paper we exploit the idea to introduce the notion of recurrences for a finite length vector $C = (C_1; \dots; C_N)$ in the Hilbert space. A distance between any vectors C^a and C^b is defined as

$$d_{ab}^2 = \int_0^1 C^a \cdot C^b = \sum_{j=1}^N \int_0^1 C_j^a \cdot C_j^b \quad (4)$$

and, particularly

$$d^2(t) = \int_0^1 C(t) \cdot C(0) \quad (5)$$

With definition (5) one can introduce a notion of the quantum recurrence (QR) as the condition

$$d_j^2(t - t_0 > 0) < \epsilon; \quad \hat{d}_j^2(t < t_0) > \epsilon; \quad (8j)$$

$$d_j = \int_0^1 C_j(t) \cdot C_j(0) \quad (8j); \quad (6)$$

Since such a definition is heuristic, it is important to see how it works and how it can distinguish between different cases, particularly between the case with classically almost uniformly mixing dynamics and the case of strongly intermittent dynamics. As an example, we consider an initial value problem for the quantum kicked rotor which, in the classical limit, is described by the standard map

$$p^0 = p + K \sin x; \quad x^0 = x + p^0; \quad p^2 = (1 - K^2)^{-1/2} p; \quad x^2 = (1 - K^2)^{-1/2} x \quad (7)$$

with a control parameter K . For $K < 1$ almost all the domain is chaotic with the Lyapunov exponent $\ln K$, excluding areas where $K \cos x_j < 1$. The marginally stable points are defined by the conditions $K = K_m = 2m$; $p = 2n$; $x = \pi n/m = 2\pi$ with integers $(m; n)$. For some $K_m \notin 0$ and the condition $0 < K - K_m < K_m$ a set of islands appears [8, 9, 10, 11] as a result of bifurcation. These islands are known as accelerator mode islands (AMI) (see more in [11, 12, 13]). The boundaries of these islands have complicated structures which can exhibit selfsimilar infinite hierarchical island chains for some specific values of the parameter K , which are known as "magic" numbers [14]. Trajectories with initial points in the inner region of the islands are trapped

inside, and at each step of the map their momentum increases by $2\hbar$ resulting in acceleration \dot{p} . Because of the island chains, these structures affect also trajectories that start in the chaotic region. Such trajectories are trapped for a long time near the island chains, and the propagation of trajectories in phase space is faster than diffusion [11, 14, 15]. As a result, anomalous superdiffusion appears. The Poincaré recurrences for the magic values of K are distributed by the power law of Eq. (3), while for $K \neq 1$ they follow the law of Eq. (1) with a high level of accuracy.

The AMI affects quantum dynamics [12, 16, 17] as well. The specific point of the present consideration is that the recurrences will be studied in the Hilbert space. We show that statistics of quantum recurrences is sensitive to the values of K , i.e., to the structural changes of phase space. Namely, emergence of the AMI due to bifurcation changes the distribution of the recurrences (6) from the exponential form similar to Eq. (1) to the power law behavior similar to Eq. (3). The following three values of the chaos parameter are chosen in the present consideration: $K = 2$; $K = 9/6$ and $K = K = 1.032 = 6.4717 \dots$. When $K = 2$ or $K = 9/6$, the AMI are absent or do not play any important role; classical chaotic dynamics corresponds to normal diffusion and statistics of the Poincaré recurrences corresponds to the exponential distribution of Eq. (1). In this case we anticipate the exponential statistics of the QR. When $K = K = 6.4717 \dots$, there are AMI [11], and one expects the power law distribution of the QR.

The quantum kicked rotor which corresponds to Eq. (7) can be defined in some dimensionless units by the Hamiltonian,

$$H = p^2/2 + K \cos x \quad (t = n); \quad (8)$$

where $p = \hbar \partial/\partial x$ is the orbital momentum for the conjugate phase x , and \hbar is the dimensionless Planck constant, while t is the time. An evolution operator over one period is

$$\hat{U} = \exp \left[\frac{p^2}{2\hbar} \right] \exp [i \cos(x)]; \quad (9)$$

where $\hbar = K/\hbar$. Let ψ_{jE} be an eigenfunction of \hat{U} with a corresponding eigenvalue E . The eigenvalue problem in the basis of eigenfunctions of the orbital momentum j reads

$$\langle m | \hat{U} | j \rangle = \sum_{m'} U_{m'j} \psi_{m'E} = e^{iE} \psi_{mj}; \quad (10)$$

where $U_{mj} = \langle m | \hat{U} | j \rangle$ and the matrix elements are

$$U_{m'j} = \langle m' | \hat{U} | j \rangle = e^{i \frac{\hbar m'^2}{2}} (i)^{m'-j} J_{m'-j}(\hbar); \quad (11)$$

where $J(z)$ is the Bessel function of the first kind [20]. We consider $\hbar = 2/M = N$ to be rational, such that the

matrix elements $U_{m'j}$ obey the following periodicity rule [18]

$$U_{m'+N, j+N} = (-1)^{m'+N} U_{m'j}; \quad (12)$$

In our consideration $U_{m'j}$ is periodic with the period N . Following [18], we present $m = s + lN$ with $0 \leq s < N$ and $l = 0, 1, \dots$. The eigenfunction, due to the Bloch theorem, is $\psi_m = \psi_{s+lN} = e^{ij} \psi_s$, where $(0 < \psi < 2\pi)$ is a quasi-momentum or Bloch vector, and ψ obeys the periodic boundary conditions $\psi_{m+N} = \psi_m$ with $\psi = 0$. Therefore, the eigenvalue problem of Eq. (10) for the infinite matrix \hat{U} is deduced to the eigenvalue problem for the finite matrix of the form [18, 19]:

$$U_{s;s^0} = \frac{1}{N} \sum_{j=1}^N \exp \left[\frac{\hbar s^2}{2} \right] \exp \left[2i \frac{(s^0 - s)j}{N} \right] \exp \left[i \cos \frac{2j}{N} \right]; \quad (13)$$

This expression for the matrix elements of the $N \times N$ matrix corresponds to the discrete Fourier inversion. Hence, the efficient way to construct $U_{s;s^0}$ numerically is using the fast Fourier transform [21].

Therefore, when \hbar is a rational with respect to 2 , namely $\hbar = 2/M = N$, the motion is realized on the extended torus $(x;p) = (2\pi/M, 2\pi/M)$. If the periodic boundary conditions are set to the wave function, the unitary evolution operator \hat{U} is reduced to a finite $N \times N$ matrix (13). We take $\hbar = 4/N$, where $N \gg 1$ and even. It enables one to keep \hbar small, and at the same time, the evolution operator \hat{U} takes the simplest form [18].

The eigenfunction ψ_E is a vector of the quasi-energy E defined in the N -dimensional Hilbert space H_N . Therefore, an arbitrary wave function, as a vector in H_N , can be defined at the initial moment $t = 0$ by the following expansion:

$$\psi(x;0) = \sum_{j=1}^N C_j \psi_{jE}(x); \quad (14)$$

where C_j are coefficients of the expansion, and these values will be defined explicitly for numerical analysis. Therefore, the evolution operator (13) determines the following wave function at the moment t

$$\psi(x;t) = \hat{U}^t \psi(x;0) = \sum_{j=1}^N C_j \psi_{jE}(x) e^{iE_j t}; \quad (15)$$

Finally, we define the distance between $\psi(x;t=0)$ and $\psi(x;t)$:

$$d^2(t) = \int_0^{2\pi} |\psi(x;t) - \psi(x;0)|^2 dx; \quad (16)$$

From Eq. (15) this reads

$$d^2(t) = 4 \sum_{j=1}^N |C_j|^2 \sin^2(E_j t) = 4 \sum_{j=1}^N |C_j|^2 d_j^2(t); \quad (17)$$

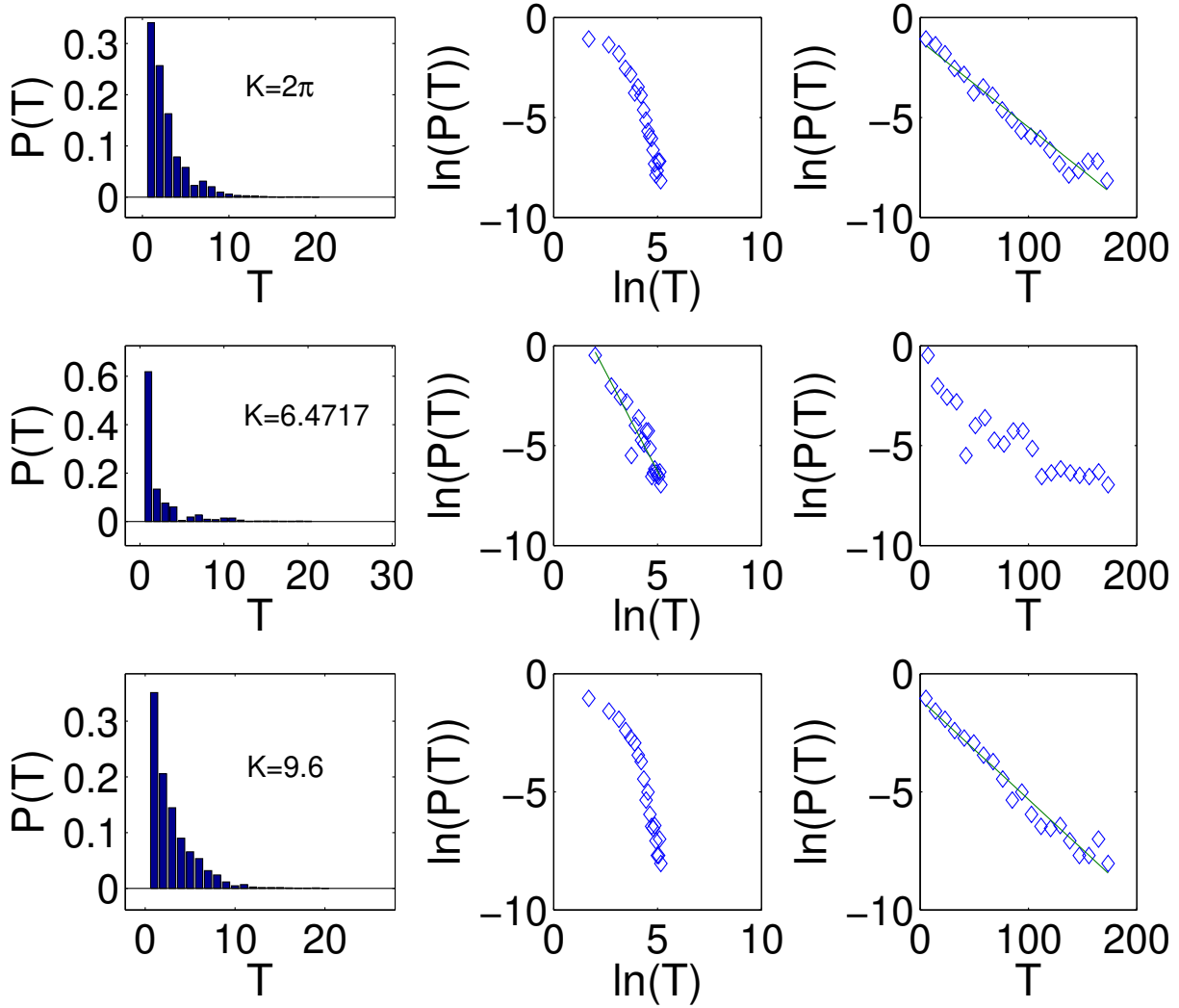


FIG. 1: Quantum recurrences distributions for 9 periods per bin for different values of K obtained after 4000 iterations. The solid lines correspond to slopes obtained by the least squares calculations.

where d_j are the same as in Eq. (6).

To study numerically the statistics of the quantum recurrences, we consider time intervals between any exit and consequent return to some cone defined in Eq. (6). We calculate times between consequent inequalities when $d_j^2(t_l) > \epsilon$ for any j and $d_j^2(t_{l+1}) < \epsilon$ for all j , and we define that $T_{\text{rec}}(l) = t_{l+1} - t_l$ is the l -th recurrence. For numerical study we take $\epsilon = 0.2$, and the coefficients \mathcal{F}_j are Gaussian functions centered at some j_0 according to

$$\mathcal{F}_j = \frac{1}{\sqrt{4\pi}} \exp[-(j - j_0)^2 / 4] \quad (18)$$

For example, when ϵ ranges from 1 to 4, only a few terms of $d_j^2(t)$ contribute to the dynamics and this makes it possible to calculate the QR times. Choosing $j_0 =$

$1; \dots; N=2$ with $N = 2^{11}$, we have reliable statistics (up to 1024) initial conditions for each ϵ . Results of numerical calculations of the distribution functions are presented in Fig. 1. The distribution functions $P(T)$ are normalized to 1 and plotted versus the recurrence cycles $T = T_{\text{rec}}$ for different values of $K = 2; 6.4717; \dots; 9.6$. We iterate 1024 initial conditions up to 4000 iterations for each ϵ which ranges in the interval $\epsilon = 1 - 4$. The distribution functions are constructed for the recurrences with cycles less than 180, since for larger cycles the statistics is poor. The distribution $P(T)$ for all three values of K is constructed for 9 cycles (recurrences) per bin. The obtained distributions are close to the distributions obtained for 4 and 6 cycles per bin. The solid lines correspond to slopes obtained by the least square calculations. This gives $b_{1=\text{rec}} = 0.0421 - 0.003$ for

$K = 9.6$ and $b_{rec} = 0.0423 - 0.003$ for $K = 2$. For these values of K well determined slopes exist for semi-log plots only, which unambiguously indicates the exponential distribution of the quantum recurrences for $K = 9.6$ and $K = 2$:

$$P(T) \sim \exp(-\beta T);$$

which is consistent with Eq. (1).

For $K = 6.4717\dots$, the well determined slope is obtained from the $\log\{\log$ plot. This is the inverse power law distribution with the recurrence exponent $\beta = 1.948 - 0.03$ (compare to Eq. (3)). It should be admitted that, although the recurrence exponent is slightly less than 2, the result does not contradict the Kac lemma (see Eq. (3)), since b_{rec} is finite in our observation, and the recurrence exponent is obtained for the initial interval which is less than 180 iterations. For example, when the cycles are considered up to 280 iterations, the recurrence exponent is larger than 2, namely: $\beta = 2.38 - 0.1$.

It is important to note that the time dependence of $d(t)$ has a deceptively simple form (17) that is similar in appearance to the evolution of a fixed sum of a stationary states. In fact, the complexity of the system, which depends on K , is hidden in the distribution of the eigenvalues E_j of the evolution operator \hat{U}^t . This means that the type of distributions $P(T)$ presented in Fig. 1 will be imposed by the distribution functions $P(\lambda)$ of the level spacings $\lambda_j = E_{j+1} - E_j$. A typical distribution $P(\lambda)$ for not so small λ

$$P(\lambda) \sim \exp(-\lambda/\lambda_0); \quad \lambda > 0 \quad (19)$$

with an appropriate value of λ_0 [22]. Here, we can state that $P(\lambda)$ also depends on the value of K or, more accurately, in the region $\lambda < \lambda_0$, $P(\lambda)$ for $K = K_1$ should have different values compared to the values of K for which the phenomenon of stickiness is not observed in classical dynamics. This property of $P(\lambda)$ is evident from our calculations (see Fig. 2). For the explanation one can recall the semiclassical derivation of the level spacing distribution obtained in [23], where sums over periodic orbits were estimated using a distribution of the Poincare recurrences. Qualitative physical consideration provides that asymptotics of $P(\lambda)$ for small λ means small frequencies or quasi-frequencies in the classical dynamics, i.e., large time for returns of trajectories to a small domain. Sticky orbits in classical dynamics have quasi-periodic returns to the sticky domain with arbitrarily long periods [1, 5]. Thus, the small λ asymptotics of $P(\lambda)$ is governed by the large T asymptotics of $P(T)$.

Statistics of the QR is also verified by calculation of the correlation dimension of the signal constructed from the set of the QR. The correlation dimension D_c of a fractional dimension manifold is constructed from the QR by a standard delay time procedure [24, 25]. For this goal, we calculate the correlation dimension

$$D_c = \lim_{\epsilon \rightarrow 1} \lim_{N \rightarrow 1} \frac{\log C(\epsilon; N)}{\log \epsilon}; \quad (20)$$

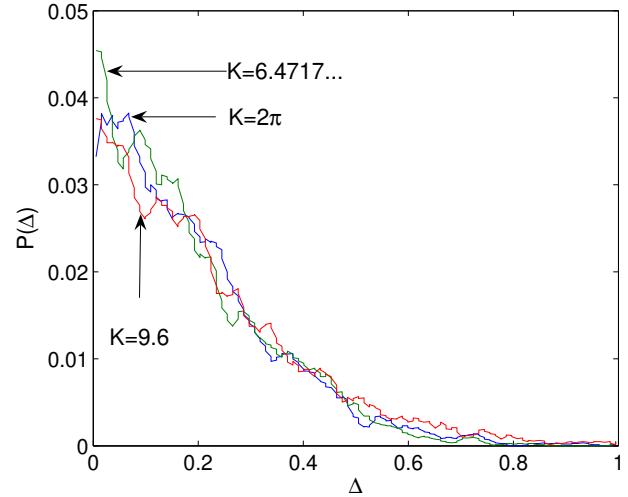


FIG. 2: Level spacing distributions

where $C(\epsilon; N)$ is a correlation integral which calculates a number of points on the fractal manifold with a distance less than ϵ . Here ϵ is the size of a cell covering the entire manifold, and N is the number of points (in our case it is a size of the QR array). The correlation integral is calculated by construction of a set of points with coordinates $x_i = (T_i; \dots; T_{i+m-1})$, where m is the dimension of the space in which the fractal manifold is embedded. Therefore the correlation integral $C(\epsilon; N)$ counts the number of points having a distance less than ϵ [24]:

$$C(\epsilon; N) = \frac{1}{N(N-1)} \sum_{i,j} \epsilon^z \mathbb{1}(\|x_i - x_j\| < \epsilon); \quad (21)$$

where $\mathbb{1}(z)$ is the Heaviside function. The result of numerical calculations is depicted in Fig. 3. The left column shows the correlation dimension as a slope calculated over the smooth parts of the curves. The right column is phase space portraits. For chaos without the AMI, when $K = 2$ or $K = 9.6$, the correlation dimensions of the QR are close to each other. Presence of the stability islands region decreases D_c by almost 3 times. This dynamical treatment of the set of QR is in complete agreement with the statistical treatment of the QR, and can be considered as an alternative method for studying quantum complexity.

In conclusion, the result of the numerical analysis is the following. The cases $K = 9.6$ and $K = 2$ correspond to the classical chaotic dynamics when the AMI are absent. In this case, the quantum recurrences in the Hilbert space has the exponential distribution. When $K = 1.03 - 2 = 6.4617\dots$, the AMI take place. The influence of these islands on both classical and quantum dynamics is essential. In the classical case, the AMI lead to superdiffusion and the power law distribution of the Poincare recurrence. In the quantum case the AMI lead to change of the QR distribution from the exponential to

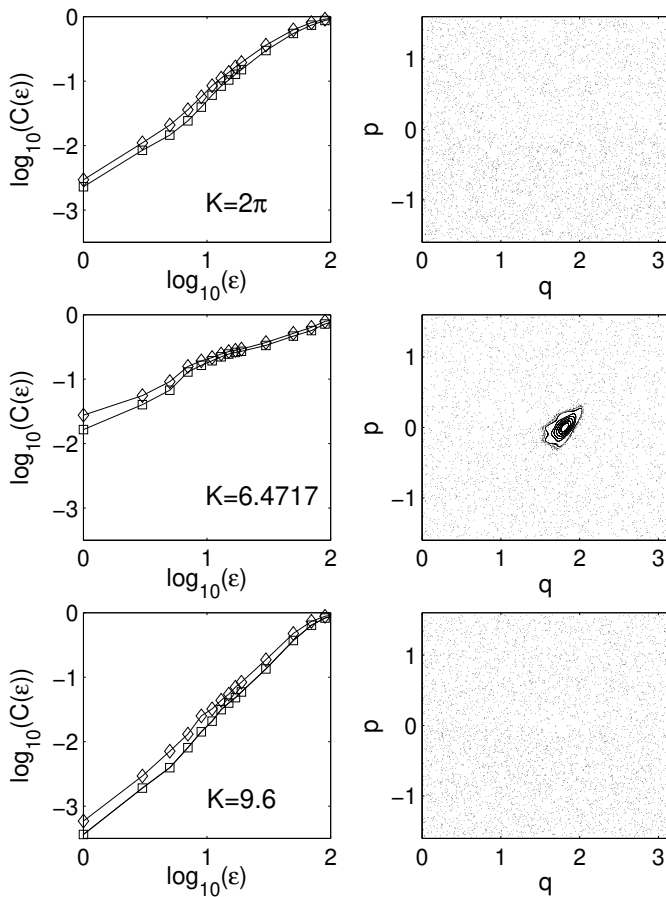


FIG. 3: Correlation dimensions D_c for different values of K . For $K = 2$, $D_c = 1.67$; for $K = 6.4717$, $D_c = 0.6$, and for $K = 9.6$, $D_c = 1.75$. These are slopes of the curves which are shown for $m = 4$ (diamonds) and for $m = 5$ (squares).

the power law.

A. I. was supported by the Israel Science Foundation and the Minerva Center for Nonlinear Physics of Complex Systems. G. M. Z. was supported by the Office of Naval Research Grants no. N00014-02-1-0056, N00014-97-1-0426.

-
- [1] G. M. Zaslavsky, *Phys. Rep.* 371, 461 (2002).
 [2] G. A. Margulis, *Functs. Ann. i Priblizh.* 3, 80 (1969); 4, 62 (1970).
 [3] M. Kac, *Probability and Related Topics in Physical Sciences.* (Interscience, New York, 1958).
 [4] J. D. Meiss, *Chaos* 7, 39 (1997).
 [5] G. M. Zaslavsky and M. K. Tippet, *Phys. Rev. Lett.* 67, 325 (1991).
 [6] V. Afraimovich and G. M. Zaslavsky, *Chaos* 13, 519 (2003).
 [7] J. H. Eberly, N. B. Narozhny, and J. J. Sanchez-Mondragon, *Phys. Rev. Lett.* 44, 1323 (1980); J. Parker and C. R. Stroud Jr., *Phys. Rev. Lett.* 56, 716 (1986); B. Yurke and D. Stoler, *Phys. Rev. Lett.* 57, 13 (1986); G. Alber, H. Ritsch, and P. Zoller, *Phys. Rev. A* 34, 1058 (1986).
 [8] C. F. F. Kamey, *Physica D* 8, 360 (1983).
 [9] V. K. Melnikov, in *Transport, Chaos and Plasma Physics, II, Proceedings, Marseille*, edited by F. Doveil, S. Benkadda, and Y. Elskens (World Scientific, Singapore, 1996), p. 142.
 [10] V. Rom-Kedar and G. M. Zaslavsky, *Chaos*, 9, 697 (1999).
 [11] G. M. Zaslavsky, M. Edelman, and B. A. Niyazov, *Chaos*, 7, 159 (1997).
 [12] J. D. Hanson, E. Ott, and T. M. Antonson, *Phys. Rev. A* 29, 819 (1984).
 [13] I. Dana, *Phys. Rev. E* 69, 016212 (2004); O. Barash and I. Dana, *Phys. Rev. E* 71, 036222 (2005).
 [14] A. Iomin and G. M. Zaslavsky, *Phys. Rev. E* 60, 7580 (1999); G. M. Zaslavsky and M. Edelman, *Chaos* 10, 135 (2000).
 [15] S. Benkadda, S. Kassibrakis, R. White, and G. Zaslavsky, *Phys. Rev. E* 55, 4909 (1997); S. Benkadda, S. Kassibrakis, R. White, and G. Zaslavsky, *Phys. Rev. E* 59, 3761 (1999).
 [16] B. Sundaram and G. M. Zaslavsky, *Phys. Rev. E* 59, 7231 (1999).
 [17] A. Iomin and G. M. Zaslavsky, *Phys. Rev. E* 63, 047203 (2001); A. Iomin, S. Fishman, and G. M. Zaslavsky, *Phys. Rev. E* 65, 036215 (2002).
 [18] S.-J. Chang and K.-J. Shi, *Phys. Rev. A* 34, 7 (1986).
 [19] F. M. Izrailev and D. L. Shepel'yansky, *Sov. Phys. Dokl.*

- 24, 996 (1979).
- [20] E. Janke, F. Emde, F. Losh, Tables of Higher Functions, McGraw Hill, NY, 1960.
- [21] R. Ketzmerick, K. Kuse, and T. Geisel, Physica D 131, 247 (1999).
- [22] F. M. Izrailev, Phys. Rep. 196, 299 (1990).
- [23] G. M. Zaslavsky, Phys. Rep. 80, 157 (1981); Sov. Phys. Usp. 16, 761 (1974).
- [24] P. Grassberger and I. Procaccia, Physica D 9, 189 (1983).
- [25] T. Sauer, Phys. Rev. Lett. 72 3811 (1994); R. Castro, T. Sauer, Phys. Rev. E 55 287 (1997).